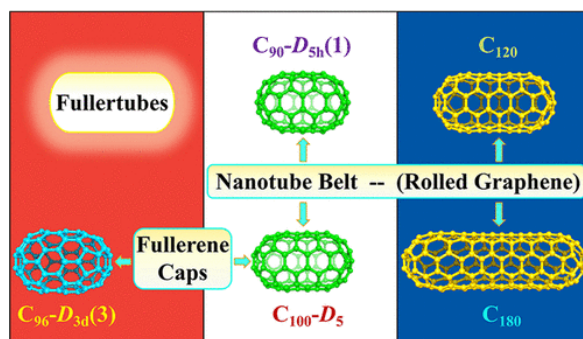


Fullertubes: Cylindrical Carbon with Half-Fullerene End-Caps and Tubular Graphene Belts, Their Chemical Enrichment, Crystallography of Pristine C_{90} - D_{5h} (1) and C_{100} - D_{5d} (1) Fullertubes, and Isolation of C_{108} , C_{120} , C_{132} , and C_{156} Cages of Unknown Structures

Ryan M. Koenig, Han-Rui Tian, Tiffany L. Seeler, Katelyn R. Tepper, Hannah M. Franklin, Zuo-Chang Chen, Su-Yuan Xie*, and Steven Stevenson*

Abstract We report a chemical separation method to isolate *fullertubes*: a new and soluble allotrope of carbon whose structure merges nanotube, graphene, and fullerene subunits. Fullertubes possess single-walled carbon nanotube belts resembling a rolled graphene midsection, but with half-fullerene end-caps. Unlike nanotubes, fullertubes are reproducible in structure, possess a defined molecular weight, and are soluble in pristine form. The high reactivity of amines with spheroidal fullerene cages enables their removal and allows a facile isolation of C_{96} - D_{3d} (3), C_{90} - D_{5h} (1), and C_{100} - D_{5d} (1) fullertubes. A nonchromatographic step (Stage 1) uses a selective reaction of carbon cages with aminopropanol to permit a highly enriched sample of fullertubes. Spheroidal fullerenes are reacted and removed by attaching water-soluble groups onto their cage surfaces. With this enriched (100–1000 times) fullertube mixture, Stage 2 becomes a simple HPLC collection with a single column. This two-stage separation approach permits fullertubes in scalable quantities. Characterization of purified C_{100} - D_{5d} (1) fullertubes is done with samples isolated in *pristine* and *unfunctionalized* form. Surprisingly, C_{60} and C_{100} - D_{5d} (1) are both *purplish* in solution. For X-ray crystallographic analysis, we used decapyrrylcorannulene (DPC). Isomerically purified C_{90} and C_{100} fullertubes were mixed with DPC to obtain black cocrystals of $2DPC\{C_{90}\text{-}D_{5h}(1)\}\cdot 4(\text{toluene})$ and $2DPC\{C_{100}\text{-}D_{5d}(1)\}\cdot 4(\text{toluene})$, respectively. A serendipitous outcome of this chemical separation approach is the enrichment and purification of several *unreported* larger carbon species, e.g., C_{120} , C_{132} , and C_{156} . Isolation of these higher cage species represents a significant advance in the unknown *experimental* arena of C_{100} - C_{200} structures. Our findings represent seminal *experimental* evidence for the existence of *two* mathematically predicted families of fullertubes: one family with an axial *hexagon* with the other series based on an axial *pentagon* ring. Fullertubes have been predicted theoretically, and herein is their experimental evidence, isolation, and initial characterization.



Introduction

The literature is plentiful for carbon nanotubes (tubular), graphene (planar), C_{60} , and C_{70} fullerenes (spheroidal).⁽¹⁾ Yet, little is known *experimentally* for soluble carbon in the range of C_{100} – C_{200} . Shown in [Figure 1](#), a **fullertube** has a well-defined and reproducible structure resembling a fullerene-capped, small radius, single-wall carbon nanotube capsule. We refer to these carbon spherocylinders as fullertubes to reflect their “part fullerene/part nanotube” regions. Fullertubes have a rolled graphene-like, tubular belt region of 6,6 ring junctions that are more chemically resistant than the reactive 5,6 ring junctions located in their end-caps. Since this “fullertube” term is new; its use henceforth will prevent confusion in future literature searches.

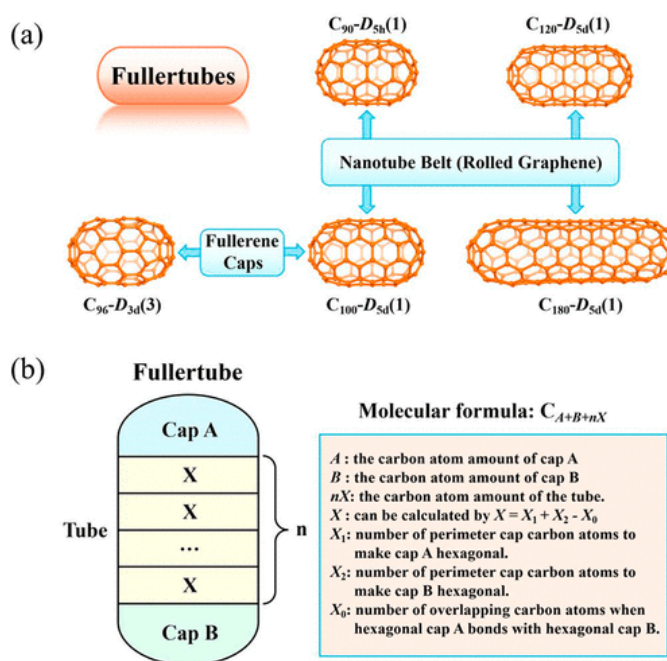


Figure 1. Fullertubes shown in (a) pristine form and as (b) C_{A+B+nX} structures with a cylindrical region bonded to end-caps, A and B. Fullertubes are reproducible structures of defined molecular weights. For IPR fullertubes, the tubular portion consists of hexagonal rings. Caps A and B each contain six isolated pentagons. Four families of fullertube listed in [Table 1](#) are exemplified in [SI Figure 1](#) for counting X_0 , X_1 , and X_2 .

The convergence of *graphene*, *fullerene*, and *nanotube* moieties into a single fullertube structure allows a unique scaffold on which to erect new 2D and 3D molecular, supramolecular, and polymeric architectures. One imagines trapping atoms or clusters inside a fullertube cavity. Likewise, derivatizing the fullertube surface would create new materials for fundamental science and applications. The rich body of work for functionalized nanotubes, fullerenes, endohedral metallofullerenes, and graphene can now be envisioned with fullertubes.

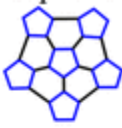

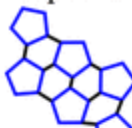
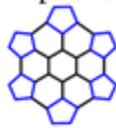
Fullertubes are defined by their two fullerene-based end-caps and tubular midsection that resemble a single layer of rolled graphene hexagons. Analogous to carbon nanotubes, the configuration of the fullertube belt can be armchair, zigzag, and a spiral loop type. Possibilities for the fullerene end-cap include the following: (1) half of a C_{60} with a pentagon-based symmetry axis (e.g., $C_{90}-D_{5h}(1)$ and $C_{100}-D_{5d}(1)$, with an armchair belt); (2) half of a C_{60} with the hexagon-based symmetry axis (e.g., $C_{96}-D_{3d}(1)$, with a zigzag belt); (3) the end-capped symmetry axis is the fusion vertex of 5,6,6 rings (with a spiral loop belt). In this latter case, the end-cap is actually the half of an oblique C_{60} . In contrast, the first two cases have an axial pentagon or an axial hexagon at the end-cap.

The unique spatial dimensions of fullertubes and their derivatives may be advantageous in biomedical research (e.g., active sites and molecular recognition). Unlike carbon nanotubes in arc-generated soot, pristine fullertubes are organic soluble and coextracted with C_{60} and C_{70} . *Advantages* of fullertubes include their reproducible structure, fixed aspect ratios (i.e., length, radius), defined molecular weights, and solubility in organic solvents without the need for polymer wrapping or chemical modification of their sidewall for dissolution.

Despite an electric-arc synthesis⁽²⁾ that emerged nearly 30 years ago, fullertubes remain a mystery and are still largely unexplored. The scarcity of fullertube research is attributed to several factors. First, there is presently a low abundance of fullertubes available in arc-generated soot extract, i.e., only 0.01–0.05% for $C_{90}-D_{5h}(1)$ and $C_{100}-D_{5d}(1)$. Second, there is no reported, efficient separation method for fullertube purification. This writing addresses this latter obstacle, although a separate work would be needed for catalyzing fullertube yields. To demonstrate the difficulty of separating fullertubes from coeluting fullerenes, for example, the isolation of $C_{90}-D_{5h}(1)$ fullertube required *four* stages of HPLC with multiple stationary phases for its purification and characterization by UV–vis and X-ray crystallography.⁽³⁾ For the $C_{96}-D_{3d}(3)$ fullertube, multiple stationary phases were again required for purification.⁽⁴⁾ Nevertheless, isolation of a chlorinated derivative of $C_{90}-D_{5h}(1)$ fullertube has led to a X-ray crystal structure.⁽⁵⁾ Likewise, a chlorination reaction was performed on a HPLC fraction containing an admixture of C_{100} -containing isomers.⁽⁶⁾ X-ray crystallography of the halogenated derivative revealed a chlorinated $C_{100}-D_{5d}(1)$ fullertube.⁽⁶⁾ Both tubular and spheroidal C_{100} fullerenes are present in arc-generated soot, but pristine and unfunctionalized $C_{100}-D_{5d}(1)$ fullertube has not yet been isolated and characterized until this work. For example, we now know that pristine $C_{100}-D_{5d}(1)$ fullertube is *purplish* in solution: a strikingly *rare* color for an all-carbon structure.

The notion of fullertubes structures is suggested based on mathematical expressions, which in turn, predicts a sequence of family members.^(7–11) For example, two fullertube families are represented by $C_{30+30+10n}$ and $C_{30+30+12n}$, where n = number of added carbon belts to the tubular portion (i.e., additional belts of carbon atoms to segmentally extend the fullertube, as shown in [SI Figure 1](#)).^(11–17) In this work, we compare our experimental findings in support of these calculated fullertube families ([Results and Discussion, Table 1](#)).

Table 1. Comparison of Literature Predicted (i.e., *Mathematical* Carbon Sequences) to Carbon Species Experimentally Observed (This Work) after Chemical Reaction with Aminopropanol

<i>Tubular IPR Series</i> $C_{30+30+10n}$ ^{11,14,16}		<i>Tubular IPR Series</i> $C_{30+30+18n}$ ^{12,17}		<i>Tubular IPR Series</i> $C_{30+30+24n}$ ^{13,17}		<i>Tubular IPR Series</i> $C_{36+36+12n}$	
Cap A=B 	Survives NH ₂ PrOH? (i.e., m/z detected) Fig. 9, S5	Cap A=B 	Survives NH ₂ PrOH? (i.e., m/z detected) Fig. 9, S5	Cap A=B 	Survives NH ₂ PrOH? (i.e., m/z detected) Fig. 9, S5	Cap A=B 	Survives NH ₂ PrOH? (i.e., m/z detected) Fig. 9, S5
C ₆₀	Yes	C ₆₀	Yes	C ₆₀	Yes	C ₇₂	No
C ₇₀	Yes	C ₇₈	Yes	C ₈₄ [#]	Yes	C ₈₄ [#]	Yes
C ₈₀	No	C ₉₆ ^{*#}	Yes, this work [†]	C ₁₀₈ [*]	Yes, this work [†]	C ₉₆ ^{*#}	Yes, this work [†]
C ₉₀ [*]	Yes, this work [†]	C ₁₁₄	Yes, this work [†]	C ₁₃₂ ^{*#}	Yes, this work [†]	C ₁₀₈ [#]	Yes, this work [†]
C ₁₀₀ [*]	Yes, this work [†]	C ₁₃₂ ^{*#}	Yes, this work [†]	C ₁₅₆ [*]	Yes, this work [†]	C ₁₂₀ ^{*#}	Yes, this work [†]
C ₁₁₀	No	C ₁₅₀ [#]	Yes, this work [†]	C ₁₈₀ [#]	Yes, this work [†]	C ₁₃₂ ^{*#}	Yes, this work [†]
C ₁₂₀ ^{*#}	Yes, this work [†]	C ₁₆₈ [#]	Yes, this work [†]	C ₂₀₄ [#]	Yes, this work [†]	C ₁₄₄	Yes, this work [†]
C ₁₃₀	Yes, this work [†]	C ₁₈₆	Yes, this work [†]			C ₁₅₆ [*]	Yes, this work [†]
C ₁₄₀	No	C ₂₀₄ [#]	Yes, this work [†]			C ₁₆₈ [#]	Yes, this work [†]
C ₁₅₀ [#]	Yes, this work [†]					C ₁₈₀ [#]	Yes, this work [†]
C ₁₆₀	No					C ₁₉₂	Yes, this work [†]
C ₁₇₀	No					C ₂₀₄ [#]	Yes, this work [†]
C ₁₈₀ [#]	Yes, this work [†]						
C ₁₉₀	No						
C ₂₀₀	No						

Appears in multiple series.

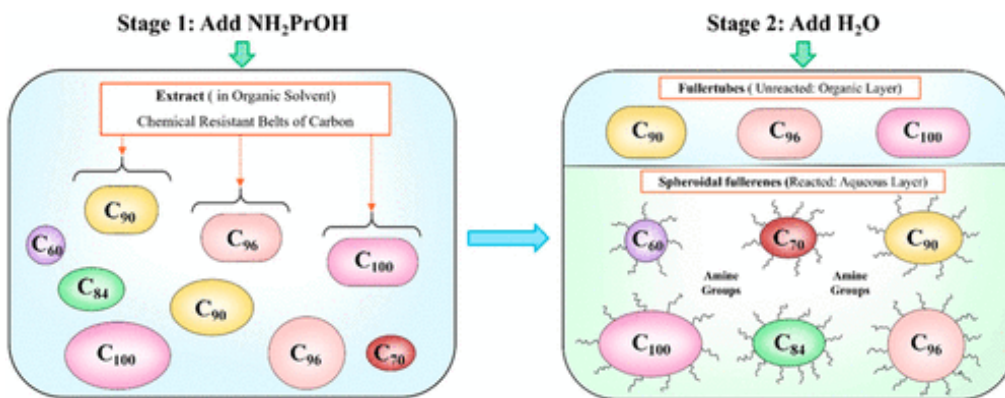
[†] The *m/z* observed experimentally (this work) in mass spectra.^{*} Isolated (this work).

Predicting the existence of fullertubes is only a first step. Experimental studies require a way to isolate them in isomeric purity *and* with sufficient quantities. For these reasons, fullertube experimental work has been stymied for nearly 30 years—with still little to no purified samples. For example, the little experimental work on fullertubes and their chlorinated derivatives includes a combination of X-ray crystallography, ¹³C NMR, and UV–vis spectroscopy.^(3–6,18,19) This paucity of fullertube literature suggests many new opportunities for seminal research.

Herein, we show how to finally isolate fullertubes in macroscopic quantities. With this chemical separation approach, isomerically pure C₁₀₀, C₉₆, and C₉₀ fullertubes are isolated in tens of milligrams when the described process is repeated with multiple batches. The chemical selectivity enriches fullertubes by factors of 100–1000 times their original abundance in extract. In this first stage, the high reactivity of primary amines with spheroidal fullerenes renders their cages hydrophilic for removal.^(20–22) (It is interesting to note that functionalized amines were used to separate metallic from semiconducting nanotubes.)^(23–27) Our second stage requires only *one* column for C₉₀, C₉₆, and C₁₀₀ fullertube isolation. HPLC purification is rapid, cost-effective, facile, and green (i.e., less solvent, less money, less time, and less chemical waste). Note: the latter half of this paper describes how our chemical approach permits the isolation of several larger and unreported carbon molecules in the C₁₀₀–C₂₀₀ range.

Scheme and Concept

As shown in [Scheme 1](#), aminopropanol selectively discriminates between tubular carbon (i.e., fullertubes) and spheroidal carbon cages (i.e., fullerenes). The basis of this separation strategy is the well-known reactivity of C₆₀ and C₇₀ with primary amines at 5,6 ring junctions.^(20,28) Fullertubes, analogous to single wall carbon nanotubes, possess a tubular region of hexagon belts with 6,6 ring junctions (i.e., less reactive to amine attack).



Scheme 1. Strategy to Chemically Separate Fullertubes from Spheroidal Fullerenes

A DFT study on the reaction of methylamine with fullerenes and carbon nanotubes shows the reactivity is dependent on the cage carbon's pyramidalization angle, which relates to the local curvature and strain at the reaction center.⁽²⁹⁾ Although methylamine was used, calculations show the addition of amine to the C₆₀ end-caps is exothermic, whereas methylamine attack on the tubular sidewall is endothermic.⁽²⁹⁾ The higher reactivity at fullerene end-caps relative to the tubular region is supported by the work of Dinadayalane et al.⁽⁹⁾ Likewise, we predict the fullertube belt to be more inert than its fullerene end-caps. As the reaction proceeds ([Scheme 1](#)), a derivatized carbon cage becomes increasingly hydrophilic, will undergo a change in solubility, and is removed with the aqueous phase in a separatory funnel. In contrast, the fullertubes (unreacted and hydrophobic) remain in the organic phase. This initial chemical precleanup (Stage 1) is a key first step *prior* to HPLC isolation (Stage 2).

Experimental Section

General

Chromatographic conditions are as follows: a pyrenyl-based stationary phase (PYE, 4.6 mm × 250 mm), mobile phase flow rate of 1 mL/min xylenes, 360 nm UV detection, and injection volumes of 50–500 μ L. Reagents and solvents were purchased new and directly used from the manufacturer. Mass spectrometry was performed on a Bruker Microflex with samples deposited on a stainless steel plate. No matrix was used (i.e., LD-TOF, positive-ion mode). UV–vis measurements were obtained with carbon disulfide as the solvent.

Feasibility and Reactivity Studies

To determine the feasibility of separating tubular and spheroidal forms of soluble carbon, 500 mg of soot extract prepared from the electric arc method⁽²⁾ was dissolved in 500 mL of toluene to achieve a concentration of 1 mg/mL. This lower solubility of 1 mg of extract per mL ensured an unsaturated solution. While stirring, 15 mL of 3-amino-1-propanol was added. To monitor the extent of reaction, aliquots of the reaction mixture were removed at different reaction times, PTFE syringe filtered, and subsequently injected for HPLC analysis.

Two-Stage Isolation of Fullertubes: Chemical Separation (Stage 1) and HPLC (Stage 2)

To prepare a sample enriched in fullertubes, we dissolved 500 mg of arc-generated soot extract in 500 mL of toluene (1 mg/mL). This solution was soaked overnight. While stirring, 15 mL of 3-amino-1-aminopropanol was added. After 1 h of vigorous stirring, the reaction mixture was allowed to settle into two layers. Containing unreacted fullertubes, the organic phase (i.e., upper layer of reaction flask) was poured into a 2-L separatory funnel containing 300 mL of deionized water. The aqueous layer (bottom) was drained to remove reacted spheroidal fullerene contaminants. The organic phase was washed five more times with distilled water, next with 200 mL of 0.1 M HCl, and then five additional times with distilled water. The organic layer was transferred to a rotary evaporator for solvent removal to provide a solid residue. Upon washing with diethyl ether, 38 mg of sample enriched in fullertubes (Stage 1) was obtained and subsequently used for HPLC fraction collection and final isolation (Stage 2).

X-ray Crystallography

The [Supporting Information](#) contains experimental details on the growth and analysis of C₉₀-D_{5h}(1) and C₁₀₀-D_{5d}(1) of crystals obtained with decapyrrylcorannulene (C₆₀H₄₀N₁₀).

Scale-Up of Fullertubes

To evaluate the scalability of Stage 1, we used a stronger solvent. Xylenes have a higher solubility of fullerenes compared to toluene. To increase the fullertube concentration (i.e., ~2 mg/mL), 2.5 g of carbon soot extract was dissolved in 1.2 L of xylenes and allowed to soak overnight. To this stirring solution, 75 mL of 3-amino-1-propanol was added. The reaction was stopped after 70 min. After settling into two phases, the organic phase (i.e., upper layer) was poured into a 2-L separatory funnel containing 300 mL of deionized water. Using the workup described above, we obtained 42 mg of a dried sample enriched in fullertubes. See [Supporting Information](#), Figure 5.

Results and Discussion

Feasibility and Reactivity Comparison

The concept of [Scheme 1](#) was evaluated on a small scale. To test our hypothesis of reactivity differences between tubular and spheroidal carbon, we dissolved 500 mg of soot extract prepared from the electric arc method([2](#)) in 500 mL of toluene. While stirring, 15 mL of 3-amino-1-propanol was added. Aliquots were taken at various reaction times and analyzed by HPLC ([SI Figure 2](#)). As shown in [Figure 2](#), a graph of the log of peak area versus time indicates that C_{60} is the most reactive, followed by C_{70} , C_{90} , C_{96} , and C_{100} . The percentage of C_{90} - $D_{5h}(1)$ and C_{100} - $D_{5d}(1)$ in the unreacted organic layer improved by two and three orders of magnitude, respectively, when compared to their original abundance in extract. Given these high enrichment levels, HPLC fraction collection becomes feasible with *baseline* resolution of C_{90} , C_{96} , and C_{100} fullertubes ([Figure 3](#)).

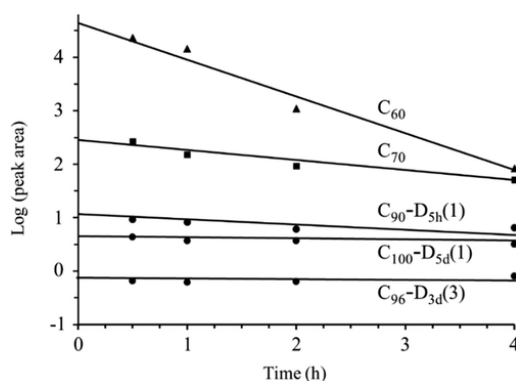


Figure 2. Comparison of reactivity differences between more reactive C_{60} and C_{70} (spheroidal) with C_{90} - $D_{5h}(1)$, C_{96} - $D_{3d}(3)$, and C_{100} - $D_{5d}(1)$ fullertubes (tubular, less reactive to amines).

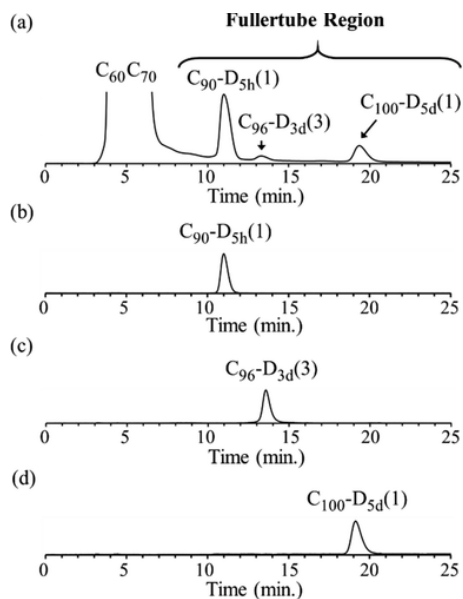


Figure 3. HPLC chromatograms for the (a) 38 mg sample of enriched fullertubes obtained after aminopropanol treatment and isolation of (b) C_{90} - $D_{5h}(1)$ fullertube, (c) C_{96} - $D_{3d}(3)$ fullertube, (d) C_{100} - $D_{5d}(1)$. HPLC conditions: PYE column, 1 mL/min xylenes, 360 nm, and 400 μ L injection.

Two-Stage Isolation of Fullertubes

Stage 1: Chemical-Based Enrichment

To obtain a sample of enriched fullertubes for HPLC separation, we dissolved another 500 mg of arc extract in 500 mL of toluene and soaked it overnight. While stirring, we added 15 mL of 3-amino-1-aminopropanol. After 1 h of reaction time, the mixture was allowed to settle. Containing unreacted fullertubes, the organic phase (i.e., upper layer of reaction flask) was poured into a separatory funnel for workup (see [Experimental Section](#)). The lower phase (aqueous) was drained to remove the, now soluble, reacted spheroidal fullerene contaminants. After solvent removal and subsequent washing of the dried residue with diethyl ether, 38 mg (isolated yield) of sample enriched in fullertubes was harvested and saved for HPLC analysis ([Figure 3a](#))

Stage 2: HPLC

Chromatographic fractions were collected for peaks eluting at 11 min ([Figure 3b](#)), 13.2 min ([Figure 3c](#)), and 19 min ([Figure 3d](#)). LDI mass spectra for the isolated species in [Figure 4](#) indicate m/z values and isotope patterns consistent with C_{90} , C_{96} , and C_{100} . ([Figure 4](#)). The isolated yield of C_{100} and C_{90} fullertube was about 2 mg for each species.

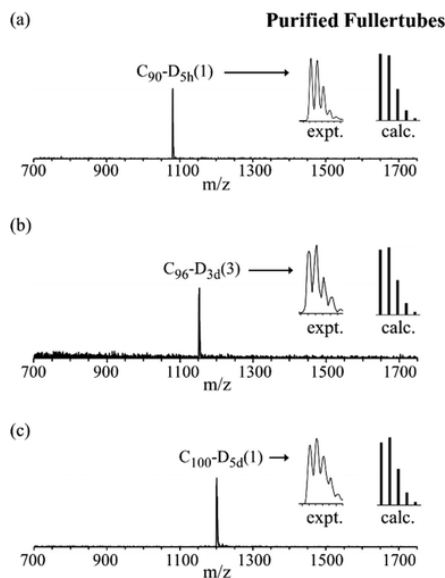


Figure 4. LDI mass spectra of (a) $C_{90}\text{-}D_{5h}(1)$, (b) $C_{96}\text{-}D_{3d}(3)$, and (c) $C_{100}\text{-}D_{5d}(1)$ fullertubes corresponding to [Figure 3](#).

UV–vis Spectroscopy of Pristine Fullertubes

Dissolved in CS_2 , purified $C_{90}\text{-}D_{5h}(1)$, $C_{96}\text{-}D_{3d}(3)$, and $C_{100}\text{-}D_{5d}(1)$ samples were characterized by UV–vis. As shown in [SI Figures 3 and 4](#), the two spectra ([Figure 5a,b](#)) for isolated C_{90} and C_{96} match those reported in the literature, whose X-ray crystallography results confirm the isomeric purity and identity of our C_{90} and C_{96} species as $C_{90}\text{-}D_{5h}(1)$ and $C_{96}\text{-}D_{3d}(3)$ fullertubes.^(3,4) Because our isolated species after chemical treatment are fullertubes (tubular), this finding supports the hypothesis that tubular carbon structures would be more resistant than spheroidal fullerenes to chemical attack of the amine. Note that we found

only one HPLC peak for C_{90} , C_{96} , and C_{100} during our fraction collection. This finding is significant because it is the first example of single pass, single column HPLC isolation of a fullertube.

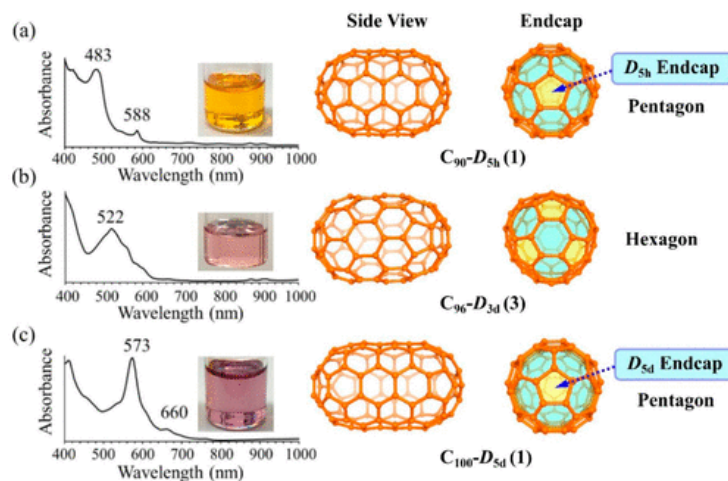


Figure 5. UV-vis spectra of chemically isolated, pristine fullertubes, (a) C_{90} - $D_{5h}(1)$, (b) C_{96} - $D_{3d}(3)$, and (c) C_{100} - $D_{5d}(1)$ dissolved in CS_2 .

Figure 5a shows a dominant peak maximum at 483 nm for the C_{90} - $D_{5h}(1)$ fullertube, which has 10 belt carbons in its tubular region. In Figure 5b, the peak maximum is red-shifted to 522 nm for the C_{96} - $D_{3d}(3)$ fullertube, which also contains belt carbons of 6,6 ring junctions in its tubular girth. For C_{100} - $D_{5d}(1)$, the peak maxima is progressively red-shifted from 483 nm (C_{90}) to 522 nm (C_{96}) to 573 nm (C_{100}), respectively (Figure 5c). Addition of a 10 carbon belt to C_{90} fullertube and slight rotation of its axial pentagon explains the conversion of C_{90} - $D_{5h}(1)$ into the C_{100} - $D_{5d}(1)$ fullertube.⁽¹⁶⁾ We could not find a UV-vis spectrum of *pristine* C_{100} - $D_{5d}(1)$ in the literature to compare with our isolated C_{100} .

The axial views for the C_{90} , C_{96} , and C_{100} fullertubes (Figure 5) reveal two types of fullertube end-caps: either pentagon-based or hexagon-based. This suggests *at least* two series of fullertubes, i.e., one family with hexagon end-caps and a second family of fullertubes having pentagon end-caps. C_{90} - $D_{5h}(1)$ and C_{100} - $D_{5d}(1)$ fullertubes are pentagon-based (Figure 5a,c). In contrast, a hexagon is the axial end-cap for the C_{96} - $D_{3d}(3)$ fullertube (Figure 5b).

An unexpected finding is the discovery that our isolated C_{100} species is purplish in solution. This is rare because the C_{100} - $D_{5d}(1)$ and the C_{60} fullerene are the only reported pristine *empty-cage* species that are purplish. The C_{96} fullerene has a purplish/peachy color. Note that most purified empty-cage fullerenes are yellow-greenish to brown when dissolved in organic solvent. Despite the C_{90} - $D_{5h}(1)$ fullertube having C_{60} -based end-caps, its solution is a dark orange.

X-ray Crystallography and Analysis of Tubular Structures

According to the spiral algorithm developed by Manolopoulos and Fowler,⁽³⁰⁾ there are 450 possible C_{100} structures that satisfy the isolated pentagon rule⁽³¹⁾ (IPR). Of these hundreds of possibilities, note that both tubular and spheroidal fullerenes are theoretical candidates. A recent study by Weis et al. performed energy calculations and reported that spheroidal shapes are increasingly favored over tubular

structures with increasing carbon number.⁽³²⁾ On the basis of the tubular X-ray crystal structure of $C_{100}-D_{5d}(1)$ fullertube in [Figure 6](#), it is clear, that experimentally, both spheroidal and tubular shapes are formed.

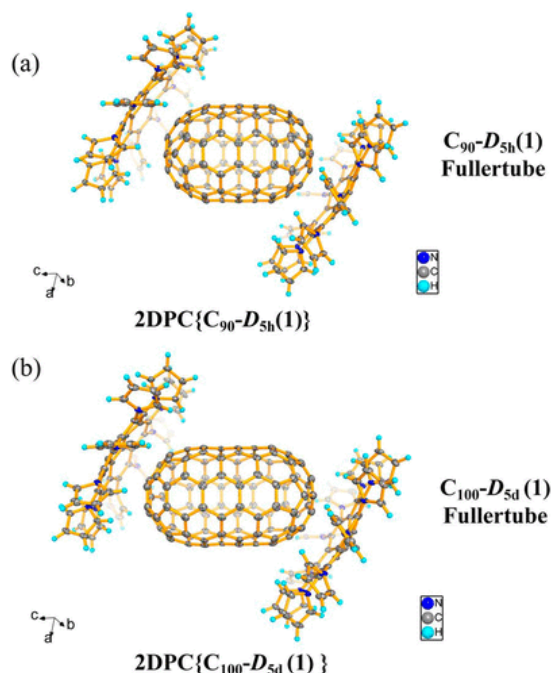


Figure 6. X-ray crystal structures of $C_{100}-D_{5d}(1)$ and $C_{90}-D_{5h}(1)$ shown with thermal ellipsoids at the 30% probability level. The toluene (solvent) in the crystal lattice is omitted for clarity.

To prove that our isolated C_{100} was indeed the $C_{100}-D_{5d}(1)$ fullertube, we successfully obtained its X-ray crystal structure. Specifically, a black, block cocrystal of $2DPC\{C_{100}-D_{5d}(1)\} \cdot 4(\text{toluene})$ [$DPC(33) = \text{decapyrrylcorannulene } (C_{60}H_{40}N_{10})$] was formed by slow evaporation after mixing together toluene solutions of $C_{100}-D_{5d}(1)$ and DPC. This same crystallization method was used to culture the supramolecular cocrystal of $C_{90}-D_{5h}(1)$ with DPC. A black cocrystal of $2DPC\{C_{90}-D_{5h}(1)\} \cdot 4(\text{toluene})$ was obtained. The structures were unambiguously identified by single-crystal X-ray diffraction. The crystallographic data are provided in [Table S1](#). Both structures of $C_{100}-D_{5d}(1)$ and $C_{90}-D_{5h}(1)$ fall into the set of fullertube structures with pentagon poles and general formula of $C_{30+30+10n}$ with D_{5h} (if n is odd, C_{90}) or D_{5d} symmetry (if n is even, C_{100}).

The asymmetric unit of $2DPC\{C_{100}-D_{5d}(1)\} \cdot 4(\text{toluene})$ consists of one-half molecule of $C_{100}-D_{5d}(1)$, one molecule of DPC, and two molecules of toluene. The asymmetric unit of $2DPC\{C_{90}-D_{5h}(1)\} \cdot 4(\text{toluene})$ consists of one-half molecule of disordered $C_{90}-D_{5h}(1)$ with the other half generated by inversion, one fully ordered molecule of DPC, and two molecules of toluene (one of the toluene species is disordered). The $C_{100}-D_{5d}(1)$ cage is fully ordered with a fullertube shape, similar to the cages in $C_{90}-D_{5h}(1)$,⁽³⁾ $La_2@C_{100}-D_5(450)$,⁽³⁴⁾ $Sm_2@C_{104}-D_{3d}(822)$,⁽³⁵⁾ $C_{100}-D_{5d}(1)Cl_{12}$.⁽⁶⁾

We find a centroid-to-centroid distance of $C_{100}-D_{5d}(1)$ between pentagons on the major axis is 11.6029 Å. This length is longer than $La_2@C_{100}-D_5(450)$ (10.083 Å) and $C_{100}-D_{5d}(1)Cl_{12}$ (11.5583 Å) as shown in [SI Figure](#)

6. Several other features of the C_{90} and C_{100} fullertube structures are noteworthy. As shown in Figure 6, the molecules of C_{100} - D_{5d} (1) and C_{90} - D_{5h} (1) are cradled by two parallel DPC molecules, respectively. Surprisingly, this orientation places two sides of C_{100} - D_{5d} (1) and C_{90} - D_{5h} (1) rather than the most curved portion of the fullerene cages adjacent to the DPC molecules. These sandwich-like conformations are different from most of the supramolecular 2DPC with V-shaped conformations reported in previous literature.⁽³³⁾ The dihedral angle between DPC plane and the major axis of C_{90} - D_{5h} (1) and C_{100} - D_{5d} (1) is approximately 56.451° and 58.241°, respectively, in the structure of 2DPC{ C_{90} - D_{5h} (1)} and 2DPC{ C_{100} - D_{5d} (1)}, respectively (see SI Figure 6).

Scale-Up of Fullertubes

To assess the feasibility of scaling-up the isolation of fullertubes, we switched from toluene to xylenes, which have higher solubility of fullerenes. For this experiment, 2.5 g of carbon soot extract was dissolved in 1.2 L of xylenes. To this stirring solution, we added 75 mL of 3-amino-1-propanol. After 70 min, the organic phase (i.e., upper layer of reaction flask) of the reaction mixture was poured into a separatory funnel for workup as described in the Experimental Section. This Stage 1 chemical procedure yielded a 42 mg sample enriched in fullertubes (SI Figure 5).

Isolation of C_{108} , C_{120} , C_{132} , and C_{156}

This 42 mg sample of enriched fullertubes was dissolved in 25 mL of xylenes, and this solution was injected into a BuckyPrep-M column (4.6 mm × 250 mm, 1.1 mL/min xylenes, 340 nm UV detection, and 500 μ L injections). Fraction collection (Figure 7a) led to HPLC purified samples of C_{108} , C_{120} , C_{132} , and C_{156} as shown in Figure 7b–e, respectively. Figure 8a–d shows the LDI mass spectral data corresponding to the samples in Figure 7. The isolated yields for C_{108} , C_{120} , C_{132} , and C_{156} were each less than 0.1 mg. The C_{90} - D_{5h} (1) and C_{100} - D_{5d} (1) peaks were also collected as described above, with isolated yields of 4 mg and 3 mg, respectively.

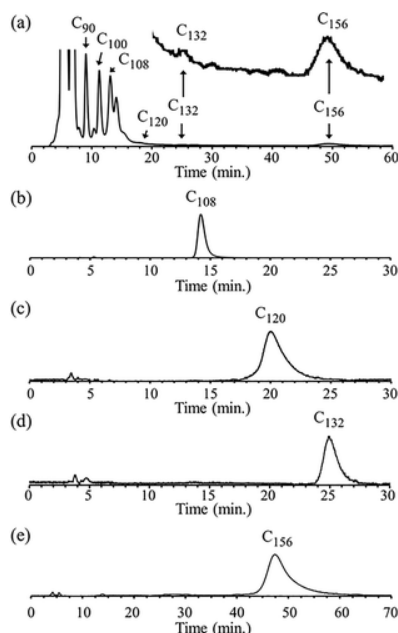


Figure 7. HPLC chromatograms obtained with a BuckyPrep-M column of (a) sample obtained after aminopropanol treatment, and isolated (b) C_{108} , (c) C_{120} , (d) C_{132} , and (e) C_{156} .

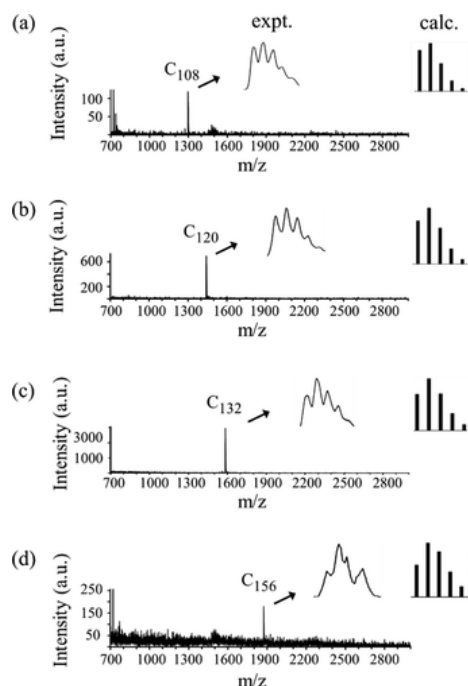


Figure 8. LDI mass spectra and isotope comparison of isolated (a) C_{108} , (b) C_{120} , (c) C_{132} , and (d) C_{156} .

Mathematical Families of Fullertubes

Looking at the mass spectra in [Figure 9](#) and [SI Figure 5](#), most fullerene structures do *not* survive the harsh reaction conditions of the aminopropanol treatment of Stage 1. Why did particular structural isomers, C_{90} (only 1 survived) C_{96} (1 survived), C_{100} (1 survived), C_{108} , C_{114} , C_{120} , C_{130} , C_{132} , C_{144} , C_{150} , C_{156} , C_{168} , C_{180} , and C_{186} , resist reaction, i.e., remain unreacted in solution while most species reacted? Is there a sequence of favored structures? Are there structural features that favor an inertness to amines? Also, note the absence of neighboring carbon peaks in the mass spectra. Specifically, why is there a mass spectral peak for C_{156} but nothing for adjacent C_{152} , C_{154} , or C_{158} fullerenes?

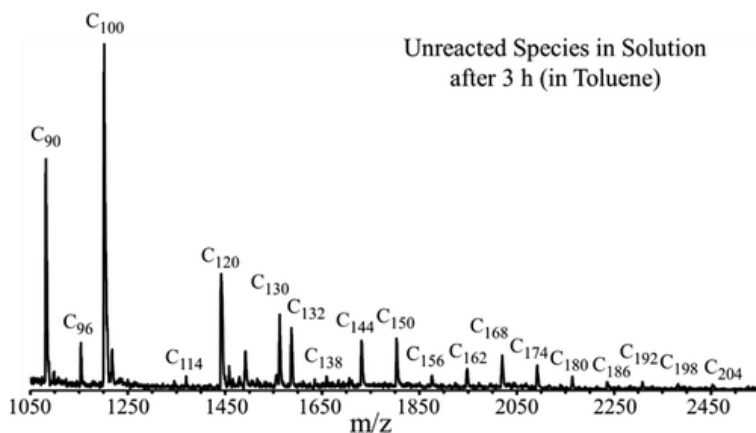


Figure 9. LDI mass spectrum of unreacted species still remaining in solution after chemical treatment with aminopropanol (see [Table 1](#) for comparison).

Mathematicians have reported several sequences of carbon structures with high symmetry.^(11,14,16) Shown in [Table 1](#), a *first* fullertube family (i.e., $C_{30+30+10n}$ series, n is the number of carbon belts) is generated with repeated additions of a 10-carbon belt to C_{60} .^(11,14,16) These calculated fullertube structures would have alternating D_{5h} and D_{5d} symmetries and consist of C_{70} , C_{80} , C_{90} , C_{100} , C_{110} , C_{120} , and so forth.^(11,14,16) A *second* tubular family of carbon has the formula, $C_{30+30+18n}$, e.g., C_{78} , C_{96} , C_{114} , C_{132} , C_{150} , C_{168} , C_{186} , and so forth.^(12,17) The *third* column in [Table 1](#) reveals a mathematical series of fullertubes; this $C_{30+30+24n}$ tubular family has a *spiral* loop of hexagons in its belt region that becomes longer as n increases. The *fourth* column shows a predicted family of carbon structures based on the formula $C_{36+36+12n}$, e.g., C_{84} , C_{96} , C_{108} , C_{120} , C_{132} , C_{144} , C_{156} , C_{168} , C_{180} , C_{192} , C_{204} , etc.).^(15–17)

By overlaying the mathematical series of fullertubes from [Table 1](#) with our mass spectral data ([SI Figures 5 and 9](#)), we can match the *experimentally observed* m/z values of surviving species with [Table 1](#)'s *mathematically predicted* families of fullertubes. For example, the carbon structures derived from the $C_{30+30+10n}$ series that *do* survive our reaction conditions include C_{120} , C_{130} , C_{150} , C_{180} , and C_{210} . In contrast, we observe no m/z peaks for carbon structures of C_{110} , C_{140} , C_{160} , C_{170} , C_{190} , and C_{200} .

Although we did isolate C_{120} ([Figure 7c](#), [Figure 8b](#)), it remains to be seen if its structure is tubular (1st column of [Table 1](#)) or spheroidal (4th column of [Table 1](#)). Given the harsh reaction conditions that removed the spheroidal fullerenes and led to the above isolated C_{90} , C_{96} , and C_{100} fullertubes, our isolated C_{120} species may likely be tubular, but the possibility of chemically stable spheroidal shape can not be ruled out at the present time. Trace amounts of isolated C_{120} hampered subsequent efforts to obtain structural information (i.e., NMR and X-ray crystallography); these types of characterization are not presently feasible.

Since C_{120} appears in *both* columns 1 and 4, it is possible that *two* structural isomers exist to explain the noticeably broad HPLC peak for C_{120} (20 min) shown in [Figure 7c](#). In comparison, HPLC peaks eluting before (C_{108}) and after (C_{132}) are both much sharper than C_{120} . The peak widths at half height for C_{108} (14 min) and for the later eluting C_{132} (25 min) are twice as narrow as the C_{120} (20 min) peak as evident in [Figure 7b,d](#). (Although the C_{156} HPLC peak in [Figure 7e](#) is also broad, this is expected based on the increased band broadening from its significantly later retention time (48 min)). The UV–vis characterization of our isolated C_{120} , C_{108} , C_{132} , and C_{156} awaits sufficient amounts necessary for X-ray crystallographic confirmation to ensure their spectra represent isomerically pure samples.

For the $C_{30+30+18n}$ mathematical series of fullertubes (second column of [Table 1](#) and examples in [SI Figure 1b](#)), we observed that m/z members of this $18n$ series *did* survive the aminopropanol reaction ([SI Figures 5 and 9](#)). This experimental data supports a possible series of tubular $C_{630+30+18n}$ species. The smallest fullertube of this family, C_{96} - $D_{3d}(3)$ fullertube, was structurally characterized by Yang et al.,⁽⁴⁾ and we show here its chemical purification ([Figure 3c](#)). The third column shows the $C_{30+30+24n}$ series ([SI Figure 1c](#)). Beginning with C_{84} , we see *experimental* evidence from these mass spectra that all m/z members of this $24n$ carbon family in [Table 1](#) survive the chemical reaction with 3-amino-1-propanol. The fourth column, $C_{36+36+12n}$, shows a series of mathematically possible family of high symmetry structures originating from a C_{72} structure ([SI Figure 1d](#)).

For our isolated larger carbon species, C_{132} and C_{156} appear in multiple columns of [Table 1](#). The small isolated amounts of purified C_{132} and C_{156} were not amenable to X-ray crystallography to determine whether their structures are spheroidal or tubular. As shown by Bodner et al.,⁽¹³⁾ there is a mathematical

family of fullertubes having a *spiral* belt of hexagons for C₁₀₈, C₁₃₂, C₁₅₆, C₁₆₈, and so forth (column 3). Our experimentally isolated C₁₀₈, C₁₃₂, and C₁₅₆ *might* correspond to these predicted spiral fullertubes.

Conclusion

We demonstrate a chemical separation approach that permits, for the first time, the isolation of several unreported, *large-size*, carbon structures in the unexplored C₁₀₈–C₁₅₆ range. We present experimental evidence in support of, not one, but *two* mathematically predicted series of fullertube: one family with a hexagonal axial end-cap and a second family having a pentagonal axial end-cap. Of significance is the matching of our experimental evidence to mathematically predicted series of fullertubes and showing that fullertube species really do *coexist* in soot with spheroidal fullerenes.

For three decades, enthusiasm for experimental studies with (1) giant fullerenes and (2) fullertubes has been difficult due to the high complexity of obtaining purified fullertubes from the abundance of contaminating, spheroidal, and structural isomers. This writing represents several advances. First, our Stage 1 chemical separation solves the HPLC coelution problem of fullertubes and fullerene structural isomers present in soot extract. Fullertubes survive our aminopropanol treatment; spheroidal fullerenes are more reactive and easily removed. From 46 possible C₉₀ IPR structures, only the C₉₀-D_{5h}(1) fullertube isomer survives. We can isolate it in milligram quantities. Of the 187 possible C₉₆ IPR structural isomers, again, only the C₉₆-D_{3d}(3) fullertube survives the reaction and is easily isolated with a single HPLC column. Likewise, of the 450 possible C₁₀₀ IPR structural isomers, only one structural isomer survives the chemical treatment with aminopropanol. We report the initial characterization of pristine C₁₀₀-D_{5d}(1) fullertube by UV–vis and X-ray crystallography. To our knowledge, this C₁₀₀-D_{5d}(1) structure is the largest and longest fullertube isolated and characterized in *pristine* and *unfunctionalized* form.

We also show the isolation of several much larger carbon structures not yet reported. Our chemical reactivity approach allows, for the first time, a facile isolation of C₁₀₈, C₁₂₀, C₁₃₂, and C₁₅₆: these four species being the largest carbon structures purified to date. Although it remains to be seen if their shapes are tubular or spheroidal, either way, this chemical purification approach permits, for the first time, access to these previously unavailable samples of “larger-size” soluble, molecular carbon.

Supporting Information

The Supporting Information is available free of charge at <https://pubs.acs.org/doi/10.1021/jacs.0c08529>.

- HPLC chromatograms, UV-vis spectra, LDI mass spectra, X-ray diffraction analysis, summary of crystallographic data ([PDF](#))
- ([CIF](#))
- ([CIF](#))

Author Information

- **Corresponding Authors**

- **Su-Yuan Xie** - *State Key Lab for Physical Chemistry of Solid Surfaces, Collaborative Innovation Center of Chemistry for Energy Materials, Department of Chemistry, College of Chemistry and Chemical Engineering, Xiamen University, Xiamen 361005, China*; <http://orcid.org/0000-0003-2370-9947>; Email: syxie@xmu.edu.cn
- **Steven Stevenson** - *Purdue University Fort Wayne, Department of Chemistry, Fort Wayne Indiana 46805, United States*; <http://orcid.org/0000-0003-3576-4062>; Email: stevenss@pfw.edu

- **Authors**

- **Ryan M. Koenig** - *Purdue University Fort Wayne, Department of Chemistry, Fort Wayne Indiana 46805, United States*
- **Han-Rui Tian** - *State Key Lab for Physical Chemistry of Solid Surfaces, Collaborative Innovation Center of Chemistry for Energy Materials, Department of Chemistry, College of Chemistry and Chemical Engineering, Xiamen University, Xiamen 361005, China*
- **Tiffany L. Seeler** - *Purdue University Fort Wayne, Department of Chemistry, Fort Wayne Indiana 46805, United States*
- **Katelyn R. Tepper** - *Purdue University Fort Wayne, Department of Chemistry, Fort Wayne Indiana 46805, United States*
- **Hannah M. Franklin** - *Purdue University Fort Wayne, Department of Chemistry, Fort Wayne Indiana 46805, United States*
- **Zuo-Chang Chen** - *State Key Lab for Physical Chemistry of Solid Surfaces, Collaborative Innovation Center of Chemistry for Energy Materials, Department of Chemistry, College of Chemistry and Chemical Engineering, Xiamen University, Xiamen 361005, China*

- **Notes** The authors declare no competing financial interest.

Acknowledgments

S.S. thanks the National Science Foundation (RUI Grant 1856461) for financial support. The National Natural Science Foundation of China (21721001) financially supports S-Y X. Project funded by China Postdoctoral Science Foundation (2020M671940) financially supports H-R.T.

References

1. Kroto, H. W.; Allaf, A. W.; Balm, S. P. C₆₀ - Buckminsterfullerene. *Chem. Rev.* 1991, 91 (6), 1213– 1235, DOI: 10.1021/cr00006a005
2. Kratschmer, W.; Lamb, L. D.; Fostiropoulos, K.; Huffman, D. R. Solid C₆₀ - A New Form of Carbon. *Nature* 1990, 347 (6291), 354– 358, DOI: 10.1038/347354a0
3. Yang, H.; Beavers, C. M.; Wang, Z. M.; Jiang, A.; Liu, Z. Y.; Jin, H. X.; Mercado, B. Q.; Olmstead, M. M.; Balch, A. L. Isolation of a Small Carbon Nanotube: The Surprising Appearance of D_{5h}(1)-C₉₀. *Angew. Chem., Int. Ed.* 2010, 49 (5), 886– 890, DOI: 10.1002/anie.200906023
4. Yang, H.; Jin, H.; Che, Y.; Hong, B.; Liu, Z.; Gharamaleki, J. A.; Olmstead, M. M.; Balch, A. L. Isolation of four isomers of C₉₆ and crystallographic characterization of nanotubular D_{3d}(3)-C₉₆ and the somewhat flat-sided sphere C₂(181)-C₉₆. *Chem. - Eur. J.* 2012, 18 (10), 2792– 6, DOI: 10.1002/chem.201103852
5. Chilingarov, N. S.; Troyanov, S. I. Unstable Isomer of C-90 Fullerene Isolated as Chloro Derivatives, C-90(1)Cl-10/12. *Chem. - Asian J.* 2016, 11 (13), 1896– 1899, DOI: 10.1002/asia.201600713
6. Fritz, M. A.; Kemnitz, E.; Troyanov, S. I. Capturing an unstable C-100 fullerene as chloride, C-100(1)Cl-12, with a nanotubular carbon cage. *Chem. Commun.* 2014, 50 (93), 14577– 14580, DOI: 10.1039/C4CC06825D
7. Achiba, Y.; Kikuchi, K.; Y, A.; Wakabayashi, T.; Miyake, Y.; Kainosho, M., Trends in Large Fullerenes: Are They Balls or Tubes? In *The Chemical Physics of Fullerenes 10 (and 5) Years Later*, W, A., Ed. Kluwer Academic Publishers: Netherlands, 1996; pp 139– 147.
8. Dresselhaus, M. S.; Dresselhaus, G.; Eklund, P. C. *Science of Fullerenes and Carbon Nanotubes*. Academic Press: San Diego, 1996.
9. Dinadayalane, T. C.; Leszczynski, J. Remarkable diversity of carbon-carbon bonds: structures and properties of fullerenes, carbon nanotubes, and graphene. *Struct. Chem.* 2010, 21 (6), 1155– 1169, DOI: 10.1007/s11224-010-9670-2
10. Chernozatonskii, L. A. Barrelenes Tubulenes - A New Class of Cage Carbon Molecules and its Solids. *Phys. Lett. A* 1992, 166 (1), 55– 60, DOI: 10.1016/0375-9601(92)90875-M
11. Verberck, B.; Tarakina, N. V. Tubular fullerenes inside carbon nanotubes: optimal molecular orientation versus tube radius. *Eur. Phys. J. B* 2011, 80 (3), 355– 362, DOI: 10.1140/epjb/e2011-10952-1
12. Bodner, M.; Bourret, E.; Patera, J.; Szajewska, M. Icosahedral symmetry breaking: C-60 to C-78, C-96 and to related nanotubes. *Acta Crystallogr., Sect. A: Found. Adv.* 2014, 70, 650– 655, DOI: 10.1107/S2053273314017215
13. Bodner, M.; Bourret, E.; Patera, J.; Szajewska, M. Icosahedral symmetry breaking: C-60 to C-84, C-108 and to related nanotubes. *Acta Crystallogr., Sect. A: Found. Adv.* 2015, 71, 297– 300, DOI: 10.1107/S2053273315003824

14. Bodner, M.; Patera, J.; Szajewska, M. C-70, C-80, C-90 and carbon nanotubes by breaking of the icosahedral symmetry of C-60. *Acta Crystallogr., Sect. A: Found. Crystallogr.* 2013, 69, 583–591, DOI: 10.1107/S0108767313021375
15. Mottaghi, A.; Ashrafi, A. R. Topological edge properties of C₆₀ + 12n fullerenes. *Beilstein J. Nanotechnol.* 2013, 4, 400–405, DOI: 10.3762/bjnano.4.47
16. Mandal, B.; Banerjee, M.; Mukherjee, A. K. Construction of planar graphs for IPR fullerenes using 5- and 6-fold rotational symmetry: some eigenspectral analysis. *Phys. Chem. Chem. Phys.* 2004, 6 (9), 2040–2043, DOI: 10.1039/b316775e
17. Mandal, B.; Datta, K.; Banerjee, M.; Mukherjee, A. K. Construction and utilisation of planar graphs of two series of IPR fullerenes through the use of threefold rotational symmetry. *Int. J. Quantum Chem.* 2005, 105 (3), 201–208, DOI: 10.1002/qua.20693
18. Bowles, F. L.; Mercado, B. Q.; Ghiassi, K. B.; Chen, S. Y.; Olmstead, M. M.; Yang, H.; Liu, Z. Y.; Balch, A. L. Ordered Structures from Crystalline Carbon Disulfide Solvates of the Nano-Tubular Fullerenes D-5h(1)-C-90 and D-5h-C-70. *Cryst. Growth Des.* 2013, 13 (10), 4591–4598, DOI: 10.1021/cg401138g
19. Wang, C. R.; Sugai, T.; Kai, T.; Tomiyama, T.; Shinohara, H. Production and isolation of an ellipsoidal C₈₀ fullerene. *Chem. Commun.* 2000, (7), 557–558, DOI: 10.1039/b000387p
20. Miller, G. P. Reactions between aliphatic amines and 60 fullerene: a review. *C. R. Chim.* 2006, 9 (7–8), 952–959, DOI: 10.1016/j.crci.2005.11.020
21. Sarina, E. A.; Mercado, B. Q.; Franco, J. U.; Thompson, C. J.; Easterling, M. L.; Olmstead, M. M.; Balch, A. L. 2-Aminoethanol Extraction as a Method for Purifying Sc₃N@C-80 and for Differentiating Classes of Endohedral Fullerenes on the Basis of Reactivity. *Chem. - Eur. J.* 2015, 21 (47), 17035–17043, DOI: 10.1002/chem.201502415
22. Stevenson, S.; Arvola, K. D.; Fahim, M.; Martin, B. R.; Ghiassi, K. B.; Olmstead, M. M.; Balch, A. L. Isolation and Crystallographic Characterization of Gd₃N@D-2(35)-C-88 through Non-Chromatographic Methods. *Inorg. Chem.* 2016, 55 (1), 62–67, DOI: 10.1021/acs.inorgchem.5b01814
23. Maeda, Y.; Kanda, M.; Hashimoto, M.; Hasegawa, T.; Kimura, S.; Lian, Y. F.; Wakahara, T.; Akasaka, T.; Kazaoui, S.; Minami, N.; Okazaki, T.; Hayamizu, Y.; Hata, K.; Lu, J.; Nagase, S. Dispersion and separation of small-diameter single-walled carbon nanotubes. *J. Am. Chem. Soc.* 2006, 128 (37), 12239–12242, DOI: 10.1021/ja063776u
24. Choi, M. S.; Yang, S. B.; Lee, M. H.; Park, S. J.; Lee, W. S.; Jung, H. T.; Choi, Y. J.; Kim, W. J. Separation of Single-Walled Carbon Nanotubes by Amine-Functionalized Polydimethylsiloxane. *Sci. Adv. Mater.* 2016, 8 (1), 171–175, DOI: 10.1166/sam.2016.2623
25. Maeda, Y.; Kimura, S.; Kanda, M.; Hirashima, Y.; Hasegawa, T.; Wakahara, T.; Lian, Y. F.; Nakahodo, T.; Tsuchiya, T.; Akasaka, T.; Lu, J.; Zhang, X. W.; Gao, Z. X.; Yu, Y. P.; Nagase, S.; Kazaoui, S.; Minami, N.; Shimizu, T.; Tokumoto, H.; Saito, R. Large-scale separation of metallic and semiconducting single-walled carbon nanotubes. *J. Am. Chem. Soc.* 2005, 127 (29), 10287–10290, DOI: 10.1021/ja051774o

26. Maeda, Y.; Komoriya, K.; Sode, K.; Kanda, M.; Yamada, M.; Hasegawa, T.; Akasaka, T.; Lu, J.; Nagase, S. Separation of metallic single-walled carbon nanotubes using various amines. *Phys. Status Solidi B* 2010, 247 (11–12), 2641– 2644, DOI: 10.1002/pssb.201000205
27. Maeda, Y.; Takano, Y.; Sagara, A.; Hashimoto, M.; Kanda, M.; Kimura, S. I.; Lian, Y.; Nakahodo, T.; Tsuchiya, T.; Wakahara, T.; Akasaka, T.; Hasegawa, T.; Kazaoui, S.; Minami, N.; Lu, J.; Nagase, S. Simple purification and selective enrichment of metallic SWCNTs produced using the arc-discharge method. *Carbon* 2008, 46 (12), 1563– 1569, DOI: 10.1016/j.carbon.2008.06.057
28. Wudl, F.; Hirsch, A.; Khemani, K. C.; Suzuki, T.; Allemand, P. M.; Koch, H. E.; Srdanov, G.; Webb, H. M., In *Fullerenes: Synthesis, Properties and Chemistry of Large Carbon Clusters*, Hammond, G. S.; Kuck, V. J., Eds. 1992; Vol. 48, pp 161– 175.
29. Lin, T. T.; Zhang, W. D.; Huang, J. C.; He, C. B. A DFT study of the amination of fullerenes and carbon nanotubes: Reactivity and curvature. *J. Phys. Chem. B* 2005, 109 (28), 13755– 13760, DOI: 10.1021/jp051022g
30. Fowler, P. W.; Manolopoulos, D. E. *An Atlas of Fullerenes*. Dover: New York, 2006.
31. Kroto, H. W. The Stability of the Fullerenes C-24, C-28, C-32, C-36, C-50, C-60 AND C-70. *Nature* 1987, 329 (6139), 529– 531, DOI: 10.1038/329529a0
32. Weis, P.; Hennrich, F.; Fischer, R.; Schneider, E. K.; Neumaier, M.; Kappes, M. M. Probing the structure of giant fullerenes by high resolution trapped ion mobility spectrometry. *Phys. Chem. Chem. Phys.* 2019, 21 (35), 18877– 18892, DOI: 10.1039/C9CP03326B
33. Xu, Y. Y.; Tian, H. R.; Li, S. H.; Chen, Z. C.; Yao, Y. R.; Wang, S. S.; Zhang, X.; Zhu, Z. Z.; Deng, S. L.; Zhang, Q. Y.; Yang, S. F.; Xie, S. Y.; Huang, R. B.; Zheng, L. S. Flexible decapyrrylcorannulene hosts. *Nat. Commun.* 2019, 10, 8343, DOI: 10.1038/s41467-019-08343-6
34. Beavers, C. M.; Jin, H. X.; Yang, H.; Wang, Z. M.; Wang, X. Q.; Ge, H. L.; Liu, Z. Y.; Mercado, B. Q.; Olmstead, M. M.; Balch, A. L. Very Large, Soluble Endohedral Fullerenes in the Series La₂C₉₀ to La₂C₁₃₈: Isolation and Crystallographic Characterization of La-2@D-5(450)-C-100. *J. Am. Chem. Soc.* 2011, 133 (39), 15338– 15341, DOI: 10.1021/ja207090e
35. Mercado, B. Q.; Jiang, A.; Yang, H.; Wang, Z. M.; Jin, H. X.; Liu, Z. Y.; Olmstead, M. M.; Balch, A. L. Isolation and Structural Characterization of the Molecular Nanocapsule Sm-2@D-3d(822)-C-104. *Angew. Chem., Int. Ed.* 2009, 48 (48), 9114– 9116, DOI: 10.1002/anie.200904662